NASA TECHNICAL MEMORANDUM

NASA TM X-67962

NASA TM X-67962

IMPORTANCE OF COMBINING CONVECTION WITH FILM COOLING

by Raymond S. Colladay
Lewis Research Center
Cleveland, Ohio

TECHNICAL PAPER proposed for presentation at
Tenth Aerospace Sciences Meeting sponsored by the
American Institute of Aeronautics and Astronautics
San Diego, California, January 17-19, 1972

IMPORTANCE OF COMBINING CONVECTION WITH FILM COOLING

by Raymond S. Colladay
National Aeronautics and Space Administration
Lewis Research Center
Cleveland, Ohio

Abstract

The interaction of film and convection cooling and its effect on wall cooling efficiency is investigated analytically for two cooling schemes for advanced gas turbine applications. The two schemes are full coverage- and counterflow-film cooling. In full coverage film cooling, the cooling air issues from a large number of small discrete holes in the surface. Counterflow film cooling is a film-convection scheme with film injection from a slot geometry. The results indicate that it is beneficial to utilize as much of the cooling air heat sink as possible for convection cooling prior to ejecting it as a film.

Introduction

The high gas temperatures and pressures expected in future gas turbine engines make convection cooling of engine components very difficult and, in some instances, impossible even for the most effective cooling configurations.[1] Under these conditions, convection cooling must be augmented by a film layer which protects the surface from the hot gas. If film cooling air is first used for convection cooling, the exit film temperature, adiabatic wall temperature, and resulting heat flux to the wall are increased over what would exist if film cooling alone were employed. The effect that the interaction of these two cooling methods has on overall cooling efficiency is of considerable importance in turbine cooling applications.

Two cooling schemes considered for advanced gas turbine applications which combine film and convection cooling are full coverage film cooling,[1,2] and counterflow film cooling.[3] In full coverage film cooling, the cooling air issues from a large number of small discrete holes in the surface. This type of cooling lies in the spectrum between pure transpiration cooling on the one end with essentially a continuous mass flux over the surface and localized film cooling on the other end. The amount of heat transferred by convection to the cooling air flowing through the wall depends on the tortuosity of the internal flow passages. The wall may be constructed of simple, straight-through holes with a low resultant convection effectiveness, or it may consist of a maze of interconnected flow passages with a relatively high convection effectiveness.

In the counterflow film cooling scheme, air flows along a convection passage on the under surface of the wall in a direction opposite to the hot gas stream and film layer then is ejected from a slot inclined at an angle to the surface. In this scheme, the degree of convection cooling can be controlled by the placement of fins in the convection passage or by allowing some of the film cooling air to bypass the convection passage.

In this paper, the importance of utilizing the heat sink available in the cooling air for convection cooling prior to ejecting it for film cooling is investigated for the full coverage and counterflow film cooling schemes.

Symbols

A	area
A_{eff}	effective area of finned surface
A_{fin}	fin area
A_p	coolant passage cross-sectional area
ADFC	adiabatic film cooling scheme - no convection cooling
b	coolant passage height
CONV	convection cooling scheme - no film cooling
C_p	specific heat
CFFC	counterflow film cooling scheme
D_h	hydraulic diameter
F	mass flux rate ratio, $\frac{G_c'}{G_g}$
FCFC	full coverage film cooling scheme
G_c	average coolant mass flux rate based on cooled surface area
G_c'	local average coolant mass flux rate
$G_{c,p}$	average coolant mass flux rate based on passage flow area
G_g	hot gas mass flux rate
h	local average reduced heat transfer coefficient - full coverage film cooling
h_c	coolant side heat transfer coefficient
h_g	local average gas-to-surface heat transfer coefficient
$\bar{h}_g$	average gas-to-surface heat transfer coefficient
h_{gx}	local gas-to-surface heat transfer coefficient
j	Colburn heat transfer factor
k	thermal conductivity
L	axial length of cooled surface area
ℓ	fin height

M	Mach number
m	slot mass flux ratio $(\rho V)_s/G_g$
$\dot{m}$	mass flow rate, ρVA
NF	number of fins per centimeter
Pr	Prandtl number
Q	heat transfer rate
q	heat flux rate
R	gas constant
Re	Reynolds number
St_g	Stanton number without blowing, $\frac{h_g}{G_g C_{p,g}}$
s	slot height
T	temperature
T_c	total coolant temperature
T_g	total gas temperature
T_{ge}	effective gas temperature (or recovery temperature)
T_{ref}	reference gas temperature
T_w	wall temperature
t	wall thickness
t_g	static gas temperature
V	velocity
x	spacial coordinate in axial direction
x_o	boundary layer development length
δ	fin thickness
η'	convection effectiveness, $\frac{T_{c,2} - T_{c,i}}{T_{w,2} - T_{c,i}}$
η_{film}	film effectiveness, $\frac{T_{ge} - T_{aw}}{T_{ge} - T_{c,2}}$
$\bar{\eta}_{film}$	average film effectiveness, $\frac{(T_{ge} - T_{aw})_{avg}}{T_{ge} - T_{c,2}}$
η_{fin}	fin effectiveness
η_o'	reference convection effectiveness
μ	viscosity
ξ	dimensionless distance, x/L
ρ	density
ϕ	temperature difference ratio, $\frac{T_{ge} - T_{w,2}}{T_{ge} - T_{c,i}}$

Subscripts:

avg	average
aw	adiabatic wall with film cooling
c	coolant
cffc	counterflow film cooling
fcfc	full coverage film cooling
g	gas
i	coolant supply condition
max	maximum
min	minimum
opf	offset plate fin
ref	reference
s	slot
T	total
uf	unfinned
w	wall
1	location at interface between coolant and wall
2	location at interface between hot gas and wall

Heat Transfer Models

Figure 1 illustrates the heat transfer models for counterflow film cooling (CFFC) and full coverage film cooling (FCFC) used in the analysis. The cooling schemes are applied to a given area of length L located a distance x_o from the apparent origin of a turbulent hydrodynamic and thermal boundary-layer on a flat plate. The local heat transfer coefficient distribution in the absence of film cooling is the same for each model.

Figure 1(a) illustrates the counterflow film cooling (CFFC) model. The coolant flows through a finned convection passage in a direction opposite to the gas stream so the convection cooling air is at its lowest temperature in the region where the film layer has decayed the most. The cooling air is ejected from a slot inclined at 30° to the surface. The containing wall forming the bottom of the convection passage was considered a structural member, insulated on the coolant plenum surface and assumed passive from a heat transfer standpoint. The outer wall thickness t and coolant passage height were assumed to be 0.05 and 0.064 centimeters, respectively.

In the full coverage film cooling (FCFC) scheme illustrated in Figure 1(b), cooling air issues from a large number of closely-spaced holes in the surface. Although only inclined holes are shown in the figure, various internal passage configurations can be considered to increase the rate of convective heat transfer to the cooling air flowing through the wall.

The wall thickness for the FCFC scheme was assumed to be equal to the combined thickness of

the outer wall and passage height of the CFFC scheme, namely 0.114 cm.

Heat Transfer Analysis

Counterflow Film Cooling Analysis

The heat transferred to a film cooled surface from the hot gas stream can be expressed in terms of the adiabatic wall temperature, T_{aw} as

$$dq_g = h_{gx}(T_{aw} - T_{w,2})dA \tag{1}$$

(All symbols are defined in the symbol list.)

Eliminating the local adiabatic wall temperature by introducing the film effectiveness, $\eta_{film} = \frac{T_{ge} - T_{aw}}{T_{ge} - T_{c,2}}$ leads to (for a unit width)

$$dq_g = h_{gx}\left[\frac{T_{ge} - T_{w,2}}{T_{ge} - T_{c,2}} - \eta_{film}\right](T_{ge} - T_{c,2})dx \tag{2}$$

The effective gas temperature T_{ge} (or the adiabatic wall temperature without film cooling or recovery temperature) is defined as $T_{ge} = t_g + \Lambda(T_g - t_g)$ with $\Lambda = Pr^{1/3}$ for turbulent flow.

The heat transferred to the coolant from a finned surface is

$$dq_c = h_c(T_{w,1} - T_c)dA_{eff} \tag{3}$$

The heat transferred to the coolant is also given by

$$dq_c = G_{c,p}A_p C_{p,c}\, dT_c = G_c C_{p,c} L\, dT_c \tag{4}$$

for a unit width. The mass velocity G_c is the average mass-flux rate based on the total cooled surface area; that is:

$$G_c = \frac{\text{Coolant flow rate}}{\text{Total cooled surface area}}$$

The local wall temperature is computed numerically by requiring a local energy balance between film cooling, wall conduction, and convection cooling that satisfies Equations (2) to (4). Wall conduction in the x-direction, as well as in the direction normal to the surface, is accounted for in the analysis.

Gas-to-surface heat-transfer coefficient. The local heat-transfer coefficient as defined by Equation (1) was assumed to be independent of blowing rate. Using the local Nusselt number correlation for a flat plate from Reference 4 with a turbulent hydrodynamic and thermal boundary-layer origin at $x = -x_o$,

$$Nu = \frac{h_{gx}x}{k} = 0.0296\, Re_x^{0.8}\, Pr^{1/3} \tag{5}$$

An x_o value of 1 centimeter was assumed in this analysis. The fluid properties in Equation (5) were evaluated at the local reference temperature given in Reference 5.

$$T_{ref} = 0.5\, T_{w,2} + 0.28\, t_g + 0.22\, T_{ge} \tag{6}$$

Values of thermal conductivity, Prandtl number, specific heat, and viscosity were obtained from Reference 6 for the combustion products of air and ASTM-A-1 fuel at a pressure of 10 atmospheres and a fuel-air ratio of 0.06.

Combining Equations (5) and (6) with Mach number, pressure, and temperature relations for a constant Prandtl number of 0.7 results in

$$h_{gx} = 0.026\, k\left[\frac{PM\sqrt{\frac{\gamma T_g}{R}}}{\mu T_{ref}\left(1 + \frac{\gamma - 1}{2}M^2\right)^{(3\gamma-1)/2(\gamma-1)}}\right]^{0.8} \times x^{-0.2} \tag{7}$$

Finned surface convection. In order to transfer enough heat to the cooling air by convection, a finned cooling passage was considered. Chosen for this study as an example of one of the more effective finned surfaces with possible application to turbine cooling is the offset rectangular plate fin shown schematically in Figure 2. The heat-transfer data for this fin configuration were obtained from Reference 7. Due to the continual interruption and reattachment of the boundary layer, the heat-transfer coefficient is of the order of twice that of an ordinary rectangular plate fin. The base conditions assumed for the fin dimensions in this study were (1) passage height b, 0.064 centimeter; (2) fin thickness δ, 0.0076 centimeter; (3) number of fins per centimeter NF, 16; and (4) a fin material of nickel.

To investigate the effect that the rate of convection cooling has on overall cooling efficiency, the coolant-side surface conductance was varied from the offset plate fin value to zero (insulated surface).

The coolant-side heat-transfer coefficient used in Equation (3) is expressed in terms of the Colburn factor j as a function of Reynolds number for the given fin configuration.(7)

$$h_c = G_{c,p}C_{p,c}j_{Pr}^{-2/3} \tag{8}$$

Air properties were obtained from Reference 6 at 10 atmospheres.

The effective surface area in Equation (3) is defined in terms of the fin effectiveness as follows:

$$A_{eff} = A_{uf} + A_{fin}\eta_{fin} \tag{9}$$

where

$$\eta_{fin} = \frac{\tanh\left(\ell\sqrt{\frac{2h_c}{k}}\right)}{\ell\sqrt{\frac{2h_c}{k\delta}}} \tag{10}$$

with

$$A_{uf} = [1 - (NF)\delta]L \tag{11}$$

$$A_{fin} = 2bL(NF) + [1 - (NF)\delta]L \qquad (12)$$

$$\ell = b + \frac{1}{2}\left(\frac{1}{NF} - \delta\right) \qquad (13)$$

for a unit width in the lateral direction.

Film effectiveness. In this study, the local variation in film temperature downstream of the slot is required in the wall energy balance. As the relatively cool film entrains hot gas from turbulent mixing at the interface, the effectiveness of the film as an insulating barrier diminishes.

Numerous investigations have been performed to measure the film effectiveness η_{film} under a variety of conditions. The η_{film} data have been correlated against the dimensionless length x/ms, and also against such additional parameters as coolant slot Reynolds number, gas Reynolds number, specific-heat ratio, and density ratio. The film effectiveness data correlated against x/ms from Reference 8 were felt to be representative for the conditions of this study.

In evaluating the coolant flow rate required to maintain the surface below a given temperature, it is more appropriate to relate the film effectiveness to the coolant flow rate per unit cooled surface area G_c than to the flow rate per unit slot area. Expressing the coolant- to gas-flow-rate ratio m in terms of G_c leads to the following expression for x/ms, which is independent of the slot height s:

$$m = \frac{(\rho V)_s}{G_g} \qquad (14)$$

where for a unit width along the slot

$$(\rho V)_s = G_c \frac{L}{S}$$

Therefore

$$\frac{x}{ms} = \frac{G_g}{G_c}\frac{x}{L} \qquad (15)$$

Numerical method. The outer wall from x = 0 to x = L was divided into a number of nodes. A numerical solution of the steady-state, two-dimensional, heat conduction equation was used to generate the wall temperature distribution satisfying an energy balance at each node. An iteration was required due to the interdependence of (1) the wall temperature distribution, (2) the coolant temperature rise through the finned passage, (3) the adiabatic wall temperature decay downstream of the slot, (4) the coolant side heat-transfer coefficient, (5) the fin effectiveness, and (6) the hot gas side heat-transfer coefficient.

The flow chart in Figure 3 gives a general outline of the program logic. The iteration loop shown in the left portion of the diagram is used to determine the coolant flow rate required to maintain a maximum surface temperature of 1255 K (1800° F). If the wall temperature distribution for a given coolant flow rate is needed, this loop is bypassed.

No wall conduction. An energy balance on a counterflow film cooled wall yields a closed form analytical expression for the average wall temperature if wall conduction is neglected. Even though conduction is important under the conditions of this study, the resulting expression is, nevertheless, useful in a qualitative sense, in providing insight into the interaction of film and convection cooling.

Equating dq_g and dq_c defined by Equations (2) and (4), respectively, assuming an average hot gas-side heat-transfer coefficient and noting that $T_{w,1} = T_{w,2} = T_w$, gives

$$\frac{G_c C_{p,c}}{h_{gx}} dT_c = (T_{c,2} - T_{ge})\left[\frac{T_{ge} - T_w}{T_{ge} - T_{c,2}} - \eta_{film}\right] d\xi \qquad (16)$$

where $\xi = x/L$. Integrating from $\xi = 0$ to $\xi = 1$, and rearranging yields the following expression for the average wall temperature

$$(T_w)_{avg} = \left(\overline{\eta}_{film} - \frac{G_c C_{p,c}}{\overline{h}_g}\right) T_{c,2} + (1 - \overline{\eta}_{film}) T_{ge} + \frac{G_c C_{p,c}}{\overline{h}_g} T_{c,i} \qquad (17)$$

Full Coverage Film Cooling Analysis

Full coverage film cooling, with cooling air ejected from a large number of small discrete holes in the surface, lies in the spectrum between pure transpiration and localized film cooling. The convection effectiveness varies depending on the internal structure of the wall.

The heat flux to a full coverage film cooled wall can be expressed in terms of a reduced heat-transfer coefficient h and the wall temperature; namely,

$$q = h_g\left(\frac{h}{h_g}\right)(T_{ge} - T_{w,2}) \qquad (18)$$

The heat-transfer coefficients h and h_g and the outer wall temperature $T_{w,2}$ are "local" averages over the surface area associated with a given injection hole. The coefficient h_g is obtained from integrating Equation (7) over the appropriate x-distance. By expressing the heat flux in this manner, it is assumed that the effective gas temperature T_{ge} is unaffected by blowing. This heat flux can also be expressed in terms of the rise in cooling air temperature as

$$q = G_c C_{p,c}(T_{c,2} - T_{c,i}) \qquad (19)$$

or in terms of the internal convection effectiveness

$$q = G_c C_{p,c}\eta'(T_{w,2} - T_{c,i}) \qquad (20)$$

where the convection effectiveness η' is a meas-

sure of the efficiency of the configuration in transferring heat to the coolant by convection.

The performance of a full coverage film cooled type wall with a large number of discretely spaced coolant ejection holes has been studied in detail for a turbine cooling application and reported in Reference 9. The wall, shown schematically in Figure 4, is composed of laminates of perforated sheet metal with injection holes typically spaced at 3 to 7 diameters in a staggered array. The following empirical relation[10] correlates heat-transfer data for a number of these laminated FCFC walls when the convection effectiveness is approximately 0.75:

$$1 - \phi = \left[1 + 0.34\left(\frac{F}{St_g}\frac{C_{p,c}}{C_{p,g}}\right)\right]^{-2.28} \qquad (21)$$

where

$$\phi = \frac{T_{ge} - T_{w,2}}{T_{ge} - T_{c,i}}$$

The dimensionless temperature difference ϕ from Equation (21) is given as a function of F/St_g $C_{p,c}/C_{p,g}$ in Figure 5. Equating the heat-flux expressions in Equations (18) and (20) and solving for the h/h_g ratio for FCFC yields

$$\frac{h}{h_g} = \frac{1 - \phi}{\phi}\,\eta'\,\frac{F}{St_g}\frac{C_{p,c}}{C_{p,g}} \qquad (22)$$

Substituting Equation (21) into Equation (22) with $\eta' = 0.75$ yields the desired reduction in the heat-transfer coefficient.

It would be desirable, however, to extend the analysis to include η' values other than the reference value of 0.75. The convection effectiveness can vary significantly depending on the extent that the back side (coolant side) of the perforated plate is augmented to allow greater surface area for increased convective heat transfer. The following method was used for extrapolation to lower values of convection effectiveness.

The heat flux to a full coverage film cooled wall can also be defined in terms of a film cooling effectiveness and h_g. With discrete coolant ejection holes, η_{film} varies locally around each hole. References 11, 12, and 13 investigate the film cooling effectiveness for one or a row of ejection holes. As with the heat-transfer coefficient, a "local" average film effectiveness η_{film} is defined for the area associated with a given injection hole. The heat flux can then be expressed as

$$q = h_g(T_{aw} - T_{w,2})$$

$$= h_g\left(\frac{T_{ge} - T_{w,2}}{T_{ge} - T_{c,2}} - \eta_{film}\right)(T_{ge} - T_{c,2}) \qquad (23)$$

Equating the heat flux given by Equation (18) with that given by Equation (23) and expressing $T_{c,2}$ in terms of the convective effectiveness and ϕ and rearranging yields,

$$\eta_{film} = \frac{\phi\left(1 - \frac{h}{h_g}\right)}{1 + \eta_o'(\phi - 1)} \qquad (24)$$

where η_o' is the reference value of the convection effectiveness at which the h/h_g ratio is known.

It was assumed that η_{film} is independent of η' for a given coolant ejection surface. This assumption is reasonable if the effect of density ratio (coolant to gas) on η_{film} is accounted for entirely through the mass flux ratio F. Equation (24) then gives,

$$\eta_{film} = f\left(\frac{F}{St_g}\frac{C_{p,c}}{C_{p,g}}\right) \qquad (25)$$

when the h/h_g ratio is substituted from Equation (22) with $\eta_o' = 0.75$. Equation (25) is plotted in Figure 6.

Finally, to obtain the functional relationship between the coolant flow rate and η', the heat flux expressions given by Equations (20) and (23) are equated yielding

$$\frac{F}{St_g}\frac{C_{p,c}}{C_{p,g}} = \eta_{film} + \frac{1}{\eta'}(\phi - \eta_{film})\frac{1}{1 - \phi} \qquad (26)$$

with η_{film} given by Equation (25).

Rearranging Equation (26), the outer wall temperature can be expressed as,

$$T_{w,2} = \left(\eta_{film} - \frac{F}{St_g}\frac{C_{p,c}}{C_{p,g}}\right)T_{c,2} + (1 - \eta_{film})T_{ge} + \frac{F}{St_g}\frac{C_{p,c}}{C_{p,g}}T_{c,i} \qquad (27)$$

the local average form of Equation (17).

Results and Discussion

In both the full coverage and counterflow film cooling schemes the convection effectiveness can vary depending on the convection passage configuration and the path the cooling air takes to the film ejection ports on the surface. The importance of maximizing the convection effectiveness within the limits of the coolant supply pressure available is discussed in this section.

Full Coverage Film Cooling

The interaction of film and convection cooling is clearly demonstrated by the wall energy balance relation (Eq. (26)) illustrated parametrically in Figure 7 for an example dimensionless wall temperature ϕ of 0.6. Two regimes, separated by a neutral curve of equal η_{film} and ϕ values, are apparent. When η_{film} is greater than ϕ, the cooling air requirements increase as the convection effectiveness increases. In this case, the film effectiveness is so high for the relatively

low blowing rate that the majority of "cooling" is accomplished by the insulation provided by the film layer and increasing the film injection temperature, $T_{c,2}$, by convection is detrimental from an overall cooling efficiency standpoint. When η_{film} is less than ϕ, increasing the convection effectiveness reduces the cooling requirements. By the following reasoning, it can be shown, however, that the full coverage film cooling scheme will always operate in the latter regime, i.e., that η_{film} is less than ϕ. Consider first the limiting adiabatic condition; the convection effectiveness η' is then zero and η_{film} and ϕ are, by definition, equal. Also, it can be seen from Figure 6, that η_{film} is less than F/St_g $C_{p,c}/C_{p,g}$. Consequently, the FCFC scheme will always operate in the region of ϕ greater than η_{film} (Fig. 7). Similarly, consider Equation (27). For given hot gas and coolant supply temperatures, allow the convection effectiveness to increase from zero without changing the film injection hole pattern. The film effectiveness remains constant but the outer wall temperature will decrease (Eq. (27)) resulting in an increase in ϕ. At any value of η' greater than zero, ϕ will be greater than η_{film}.

When the outer wall temperature is maintained at a specified level (corresponding to a fixed value of ϕ if T_{ge} and $T_{c,i}$ are held constant), and the convection effectiveness is increased keeping the film injection hole array fixed, the wall will not respond along the constant η_{film} curves in Figure 7. As the blowing rate decreases, η_{film} also decreases following the relation given by Figure 6.

Including this dependence of η_{film} on the blowing rate, parametric curves of constant ϕ from Equation (26) are plotted in Figure 8. It should be emphasized that since the data used in generating the curve in Figure 6 is for a staggered hole array of 3 to 7 diameter spacing the ϕ curves in Figure 8 correspond to that injection hole pattern. For the fixed injection hole configuration, the back-side (coolant-side) of the perforated plate is augmented to allow greater surface area for increased convection.

The curve for dimensionless temperature ϕ equal to 0.6 is given in Figure 9 for hot gas conditions of 20 atmospheres total pressure, 1667 K (3000° F) effective gas temperature, and 0.6 Mach number, and a coolant supply temperature of 811 K (1000° F). The cooling air required to maintain an outer wall temperature of 1225 K (1800° F) can be greatly reduced by designing an inside wall configuration which will allow high rates of convection cooling. A simple perforated plate which has an η' value of about 0.2 (typical of a wall with straight holes and plenum supplied cooling air) would require more than twice the cooling air as a wall having the same injection hole array but with a convection effectiveness of 0.75; the latter being typical of the laminate perforated plates (Lamilloy).

Figure 10 summarizes the effects of combining film and convection cooling in series for the full coverage film cooling scheme. The independent variable in the figure is the convection effectiveness with the F/St_g $C_{p,c}/C_{p,g}$ versus η' curves on the left. The corresponding η_{film} curves, related to the constant ϕ curves by a common value of F/St_g $C_{p,c}/C_{p,g}$ appear on the right. For example, with a convection effectiveness of 0.6, the FCFC wall would require a blowing parameter value of 1.6 for a dimensionless temperature difference ϕ of 0.6. Reading across to the η_{film} curve at the given value of F/St_g $C_{p,c}/C_{p,g}$ the corresponding film effectiveness is 0.26. If the convection effectiveness is reduced, the coolant mass flux rate must increase to maintain the required surface temperature. The increased blowing rate simultaneously increases the film effectiveness which reduces the sensitivity of F/St_g $C_{p,c}/C_{p,g}$ to η' from what would otherwise exist in the absence of film cooling. Note that when η' is zero, ϕ is equal to η_{film} and that η_{film} is always less than ϕ for nonzero values of η'.

Counterflow Film Cooling

Typical outer wall and cooling air temperature distributions for the CFFC scheme are shown in Figure 11 for a surface 4 cm in length. All of the results for the CFFC scheme are illustrated for example conditions of 20 atmospheres total gas pressure, 1667 K (3000° F) effective gas temperature, 0.6 gas Mach number, and 811 K (1000° F) coolant supply temperature. It should be understood that the basic conclusions related to the interaction of film and convection cooling are not unique to these example conditions. The surface temperature distribution exhibits a maximum at a point between the convection passage inlet and the film slot due to the counterflow directions of the convection air and film layer. In the region to the left of the maximum, film cooling plays the major role, and to the right, convection cooling dominates. By properly balancing the two cooling mechanisms, the maximum temperature variation can be minimized.

The advantage of combining film and convection cooling is evident from Figure 12 which compares the CFFC wall (repeated from Fig. 11) with the wall temperature distribution which would exist if the wall were cooled by (1) film cooling only - adiabatic wall (ADFC), and (2) convection only with no film cooling (CONV). The coolant flow rate is the same for all three cooling schemes. The direction of coolant flow for the CONV scheme is opposite that of CFFC since the convection passage inlet end would customarily be located in the region of highest heat flux.

As in the FCFC case, the conservation of energy relations for the counterflow film cooling scheme indicates that it is beneficial to utilize as much of the heat sink available in the cooling air for convection cooling as possible before ejecting it as a film. A reduction in the rate of convection cooling results in an increase in the maximum and average outer wall temperature for a fixed coolant flow rate as shown in Figure 13. In this figure, the overall finned surface conductance is reduced uniformally over the passage length from that of the offset plate fin to zero (adiabatic wall) while maintaining a constant coolant flow rate. The bounding dashed curves are repeated from Figure 12.

An alternative demonstration of the importance of convection cooling to the counterflow film cooling scheme is illustrated in Figure 14 where a per-

centage of film cooling air is allowed to bypass the convection passage. The maximum and average wall temperature and maximum surface temperature difference increases when some of the film cooling air is allowed to pass directly out of the film slot even though the exit film temperature, $T_{c,2}$, and resultant heat flux to the wall decreases.

It is apparent from these results that film and convection cooling must be combined for effective utilization of cooling air and moreover, the rate of convection cooling should be maximized within the limits of the pressure drop available.

Concluding Remarks

In the high gas temperature and pressure environments expected in future gas turbine engines, convection cooling of turbine components must be augmented by film cooling for efficient use of cooling air. It is beneficial to utilize as much of the heat sink available in the cooling air as possible for convection cooling before ejecting it as a protective film. Increasing the rate of convection cooling prior to film ejection reduces the cooling air required to maintain a given average wall temperature even though the exit film temperature, adiabatic wall temperature, and resulting heat flux to the wall increases.

References

1. Esgar, J. B., Colladay, R. S., and Kaufman, A., "An Analysis of the Capabilities and Limitations of Turbine Air Cooling Methods," TN D-5992, 1970, NASA, Cleveland, Ohio.

2. Livingood, J. N. B., Ellerbrock, H. H., and Kaufman, A., "1971 NASA Turbine Cooling Research Status Report" (proposed NASA Memorandum).

3. Colladay, R. S., "Analysis and Comparison of Wall Cooling Schemes for Advanced Gas Turbine Applications," (proposed NASA Technical Note).

4. Kays, W. M., Convective Heat and Mass Transfer, McGraw-Hill, New York, 1966.

5. Eckert, E. R. G., and Drake, R. M., Jr., Heat and Mass Transfer, 2nd ed., McGraw-Hill, New York, 1959.

6. Poferl, D. J., Svehla, R. A., and Lewandowski, K., "Thermodynamic and Transport Properties of Air and the Combustion Products of Natural Gas and of ASTM-A-1 Fuel with Air," TN D-5452, 1969, NASA, Cleveland, Ohio.

7. London, A. L., and Shah, R. K., "Offset Rectangular Plate-Fin Surfaces--Heat Transfer and Flow Friction Characteristics," Journal of Engineering for Power, Vol. 90, No. 3, July 1968, pp. 218-228.

8. Hartnett, J. P., Birkebak, R. C., and Eckert, E. R. G., "Velocity Distributions, Temperature Distributions, Effectiveness and Heat Transfer for Air Injected Through a Tangential Slot Into a Turbulent Boundary Layer," Journal of Heat Transfer, Vol. 83, No. 3, Aug. 1961, pp. 293-306.

9. Nealy, D. A., and Anderson, R. D., "Heat Transfer Characteristics of Laminated Porous Materials," EDR-5856, AFAPL-TR-68-98, AD-391895, Aug. 1968, General Motors Corp., Indianapolis, Ind.

10. Anderson, R. D., Davis, W. C., McLoed, R. N., and Nealy, D. A., "High Temperature Cooled Turbine Blades." EDR-6176, AFAPL-TR-69-41, AD-504209L, May 1969, General Motors Corp., Indianapolis, Ind.

11. Goldstein, R. J., Eckert, E. R. G., and Ramsey, J. W., "Film Cooling with Injection Through a Circular Hole," HTL-TR-82, NASA CR-54604, May 1968, University of Minnesota, Minneapolis, Minn.

12. Goldstein, R. J., Eckert, E. R. G., Eriksen, V. L., and Ramsey, J. W., "Film Cooling Following Injection Through Inclined Circular Tubes," HTL-TR-91, NASA CR-72612, Nov. 1969, University of Minnesota, Minneapolis, Minn.

13. Ramsey, J. W., and Goldstein, R. J., "Interaction of a Heated Jet with a Deflecting Stream," HTL-TR-92, NASA CR-72613, Apr. 1970, University of Minnesota, Minneapolis, Minn.

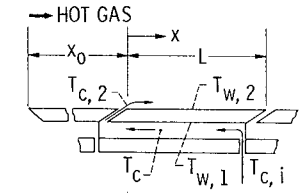

(a) Counterflow film cooling (CFFC).

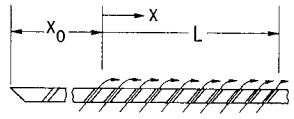

(b) Full-coverage film cooling (FCFC).

Figure 1. - Heat-transfer models.

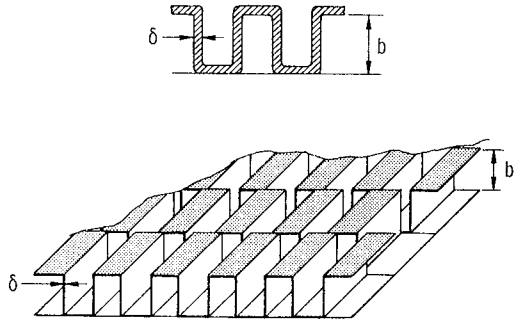

Figure 2. - Offset rectangular plate fin configuration.

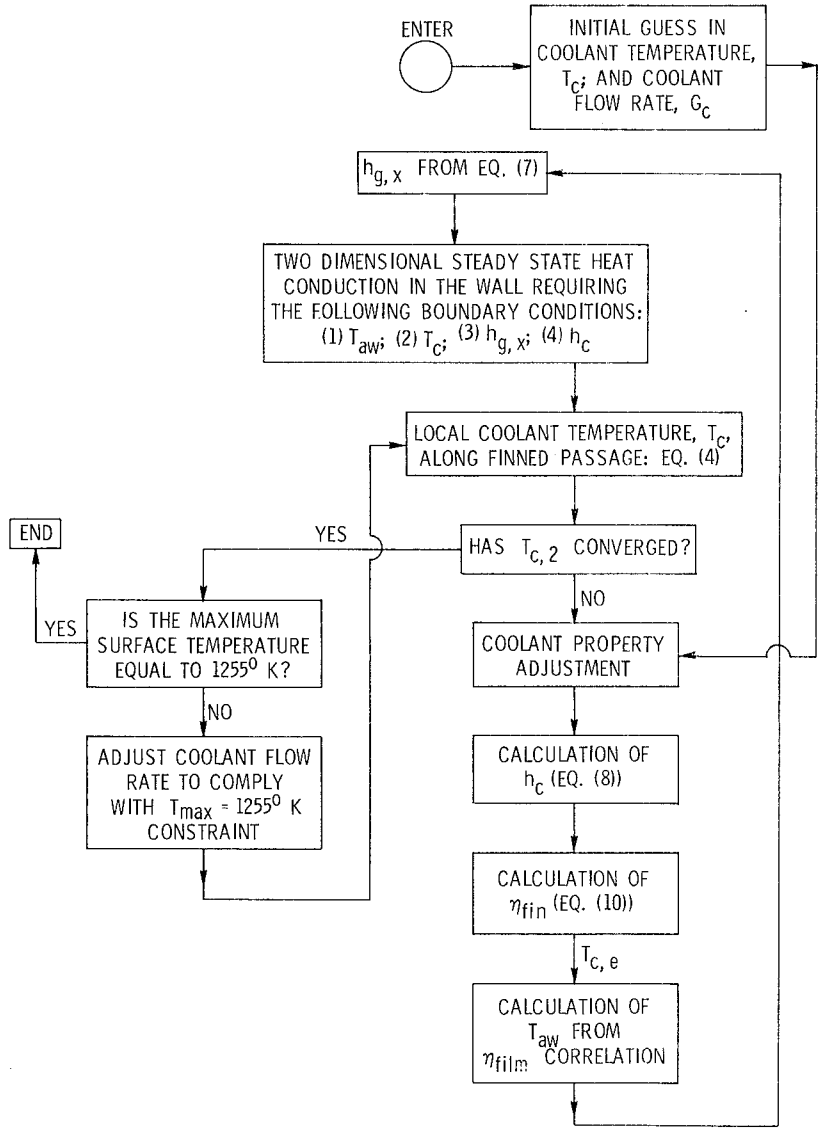

Figure 3. - Flow chart describing program logic.

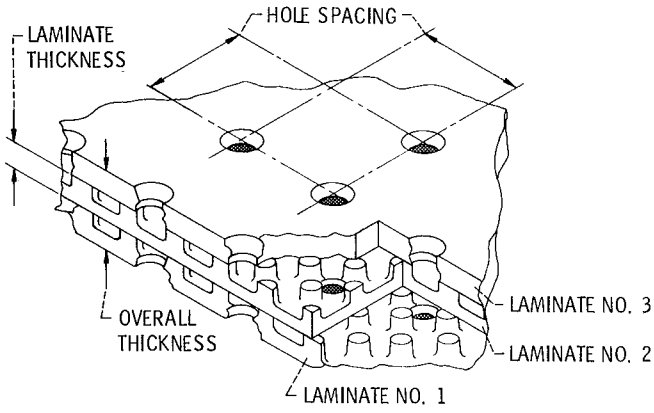

Figure 4. - Typical laminated wall configuration.

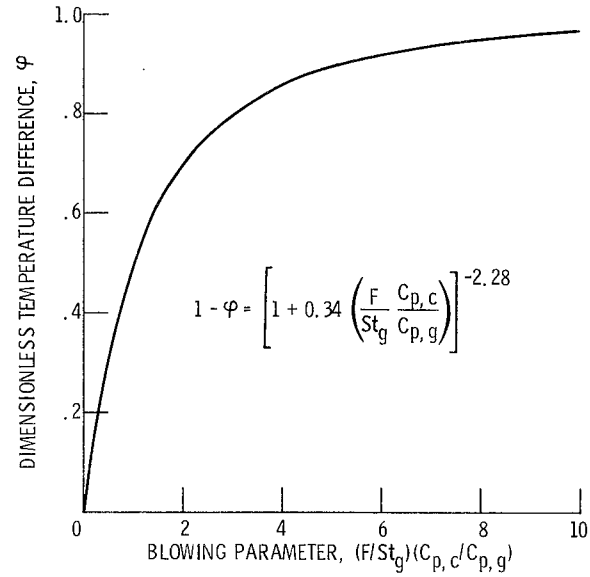

Figure 5. - Dimensionless temperature correlation for full coverage film cooled laminated plate wall from reference 10.

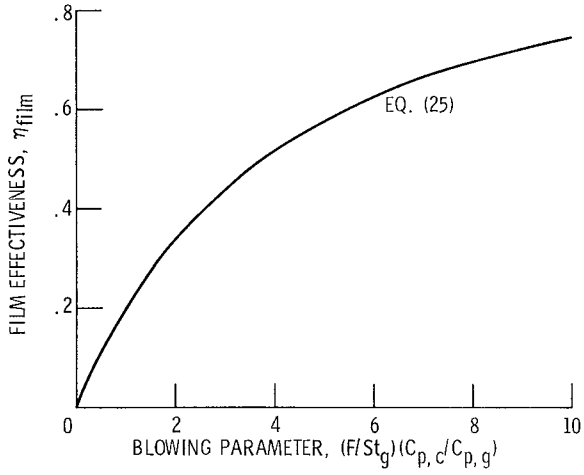

Figure 6. - Average film effectiveness for a full coverage film cooled wall with staggered film injection holes spaced at 3 to 7 diameters.

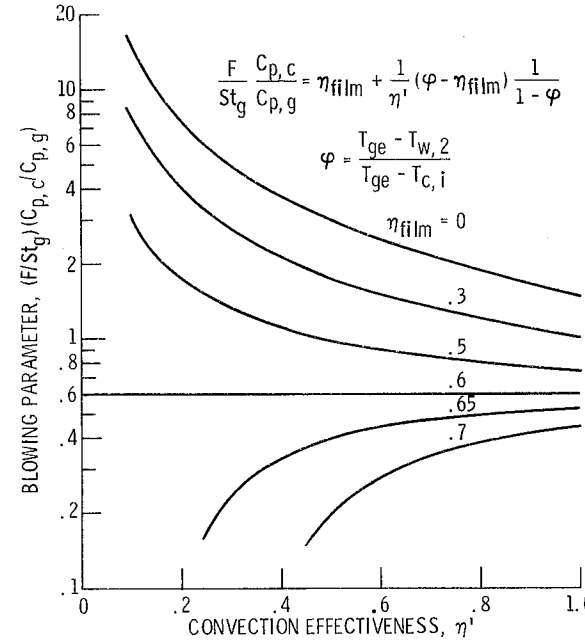

Figure 7. - Interaction of film and convection cooling with parametric curves of constant film effectiveness. Full coverage film cooling. Overall cooling efficiency, $\varphi = 0.6$.

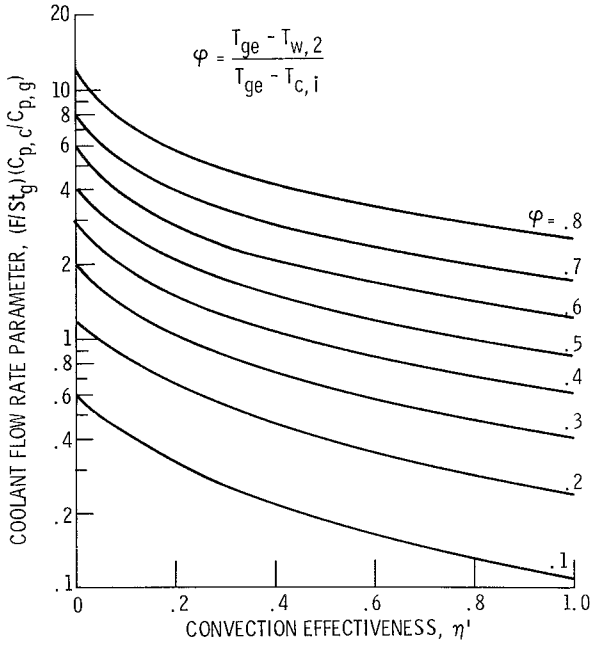

Figure 8. - Overall cooling efficiency of a full coverage film cooled wall of fixed injection hole pattern as a function of convection effectiveness.

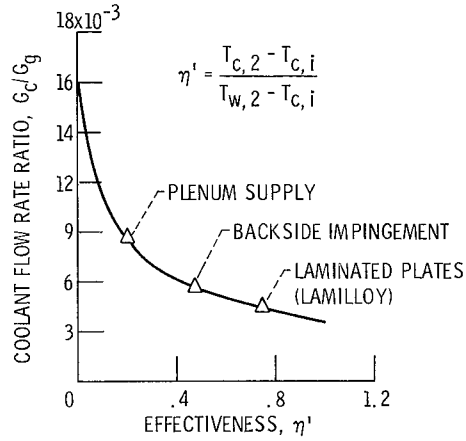

Figure 9. - Influence of convection effectiveness on cooling air requirements for a full coverage film cooled wall of fixed injection hole pattern. Total gas pressure, 20 atmospheres. Effective gas temperature, 1667 K (3000° F). Average outer wall surface temperature, 1255 K (1800° F). Coolant supply temperature, $T_{c,i}$, 811 K (1000° F). Dimensionless temperature difference φ, 0.6.

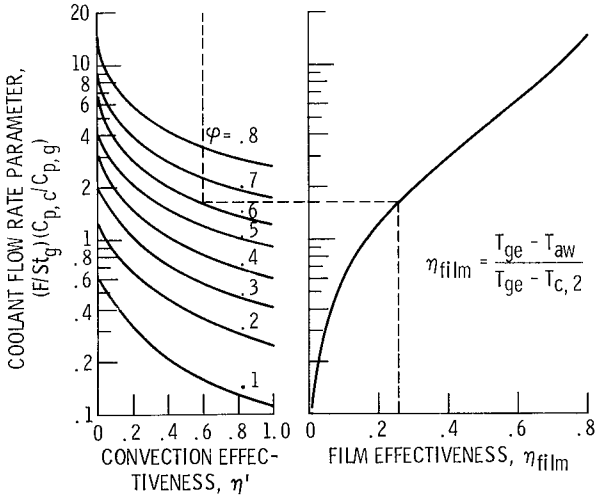

Figure 10. - Interaction of film and convection cooling in a full coverage film cooled wall of fixed injection hole pattern.

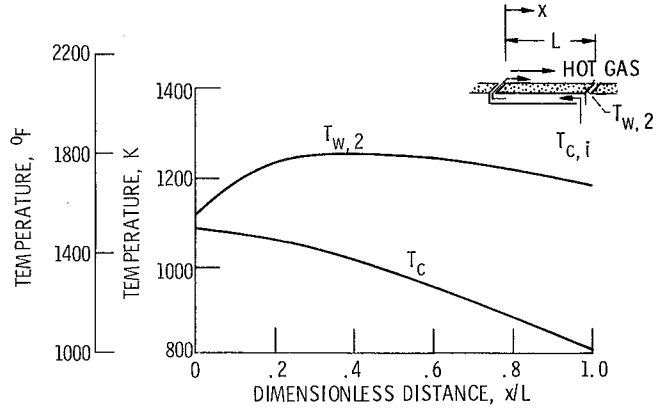

Figure 11. - Typical wall and cooling air temperature distributions for the counterflow film cooling scheme.

E-6439

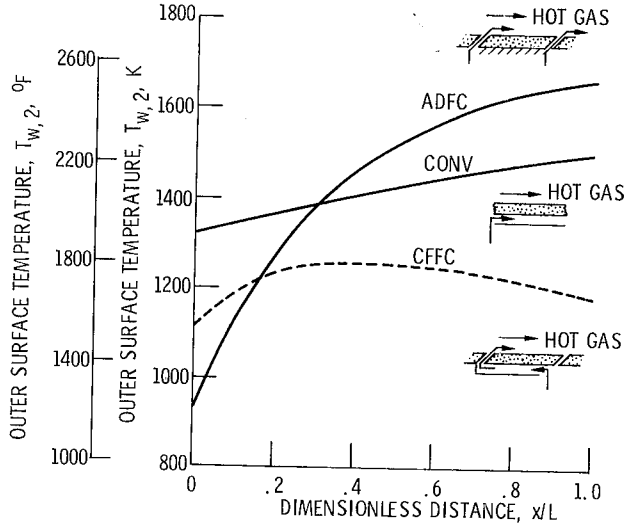

Figure 12. - Effect of combining film and convection cooling. Constant coolant flow rate.

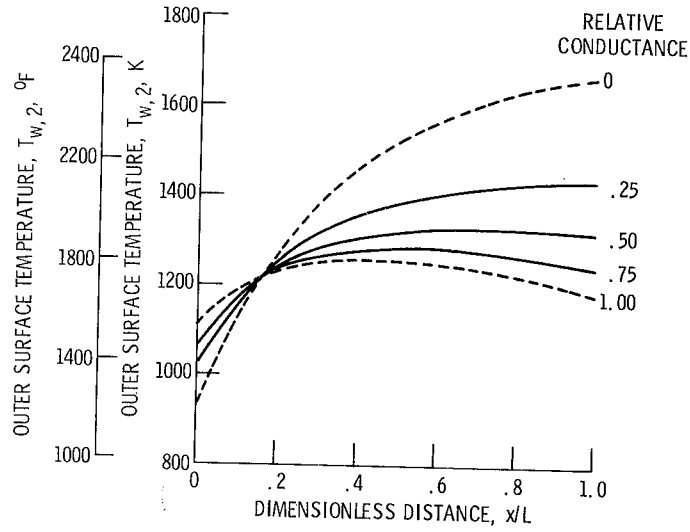

Figure 13. - Effect of convection cooling on the surface temperature distribution of a counterflow film cooled wall. Reference conductance corresponds to offset plate fin surface. Constant coolant flow rate.

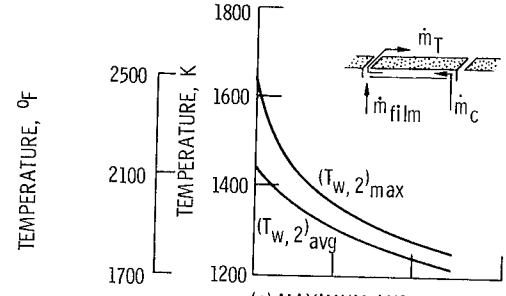

(a) MAXIMUM AND AVERAGE SURFACE TEMPERATURE.

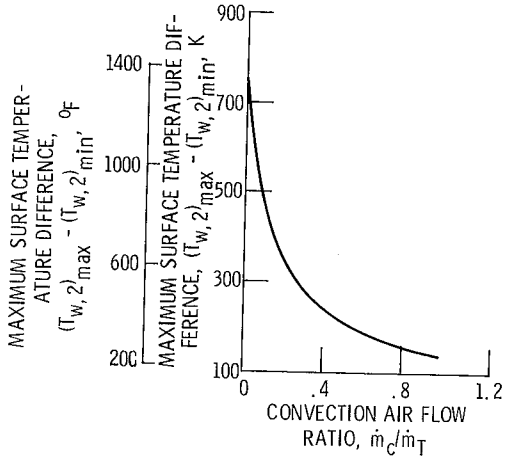

(b) MAXIMUM SURFACE TEMPERATURE DIFFERENCE.

Figure 14. - Effect of reducing the percentage of total film cooling air used for convection cooling in the counterflow film cooling scher